www.sciencemag.org/content/358/6366/1078/suppl/DC1

Supplementary Materials for

Creation of a Bose-condensed gas of ^{87}Rb by laser cooling

Jiazhong Hu,*† Alban Urvoy,* Zachary Vendeiro, Valentin Crépel, Wenlan Chen, Vladan Vuletić†

*These authors contributed equally to this work.
†Corresponding author. Email: jiazhong@mit.edu (J.H.); vuletic@mit.edu (V.V.)

Published 24 November 2017, *Science* **358**, 1078 (2017)
DOI: 10.1126/science.aan5614

This PDF file includes:

Materials and Methods

Experimental details

The two trapping beams differ in frequency by 160 MHz to avoid interference effects and their powers can be independently controlled by separate acousto-optic modulators. The intensity of the circularly polarized optical pumping beam on the D_1 transition at 795 nm is set to an off-resonant scattering rate $\Gamma_s \sim 2 \times 10^3$ s^{-1} for the $|F = 2, m_F = 1\rangle \rightarrow |F = 2, m_F = 2\rangle$ transition at a detuning $\Delta_2/(2\pi) = -630$ MHz. An electro-optic modulator generates sidebands at 6.8 GHz, and the power ratio between the two frequency component is set to have a 3 times stronger scattering rate on the $|F = 1, m_F = 1\rangle \rightarrow |F = 2, m_F = 2\rangle$ transition. This prevents the atoms that have decayed to the $|F = 1\rangle$ state from undergoing heating Raman transitions. The atoms are imaged after a time-of-flight of typically 1.3 ms via absorption imaging on the cycling transition of the D_2-line, in the plane defined by the lattice beams, and at a 20° angle relative to the X lattice beams (see Fig. 1 of the main text). We summarize the relevant experimental parameters in Table S1.

Estimation of the phase space density $\mathcal{D}$

We measure the kinetic energies K_{xy} and K_z, and compare them to the trapping vibrational frequencies ω_{xy} and ω_z. Hence, we estimate the relative ground state occupation along each direction when the chemical potential is zero. Assuming T_β ($\beta = x$, y or z) is the temperature along direction β with the vibrational frequency ω_β, the kinetic energy K_β is related to T_β by

$$K_\beta = \frac{1}{4}\hbar\omega + \frac{1}{2}\hbar\omega \frac{1}{e^{\frac{\hbar\omega_\beta}{k_B T_\beta}} - 1}. \tag{S1}$$

Then, we know the relative ground state occupation is

$$p_{0,\beta} = 1 - e^{-\frac{\hbar\omega_\beta}{k_B T_\beta}} = \frac{2}{\frac{4K_\beta}{\hbar\omega_\beta} + 1}. \tag{S2}$$

The occupation of the 3D ground state is

$$P_0 = p_{0,x}p_{0,y}p_{0,z} = \frac{2}{\frac{4K_z}{\hbar\omega_z}+1}\left(\frac{2}{\frac{4K_{xy}}{\hbar\omega_{xy}}+1}\right)^2. \tag{S3}$$

Thus the phase space density $\mathcal{D}$ is calculated as

$$\mathcal{D} = N_1 P_0 = N_1 \frac{2}{\frac{4K_z}{\hbar\omega_z}+1}\left(\frac{2}{\frac{4K_{xy}}{\hbar\omega_{xy}}+1}\right)^2 \approx N\frac{\hbar\omega_z}{k_B T_z}\left(\frac{2}{\frac{4K_{xy}}{\hbar\omega_{xy}}+1}\right)^2, \tag{S4}$$

here $T_z = 2K_z/k_B \gg \hbar\omega_z/k_B$ is the measured temperature along z. $K_x = K_y = K_{xy}$ is the measured kinetic energy along x or y, and N_1 is the peak atom number per lattice tube.

Gaussian fit to the wings of the distribution

After we measure the velocity distribution of the ballistic expansion, we choose two lines (dashed orange in Fig. S1) on the slopes of the distributions, separating the central peak and the wings parts. These two lines are fixed for all the measurements with 1.3 ms expansion time. We fit a Gaussian function (red solid lines) to the data points lying outside of the two lines. Then we subtract the fitted Gaussian function from the data points to fit a non-negative quadratic function and add it to the top of the Gaussian fit (green solid lines).

Three-body recombination measurement

It was previously reported that three-body losses are strongly reduced in a one-dimensional cloud (*27, 28*). Indeed we are not able to measure any significant three-body loss in the tubes. Therefore we measured the three-body recombination rate in a two-dimensional geometry by transferring the atoms to the Y optical lattice (i.e. by merging the tubes in the x direction) after the final cooling for 10 ms, and measuring the atom number as a function of the holding time (Fig. S2).

By fitting the theoretical model for the three-body loss, we obtain an initial loss timescale of $\tau = 300$ ms. Assuming a thermal velocity distribution for the atoms and averaging over the

Gaussian density profile in each trap and over the different lattice sites in the 1D lattice, we obtain the following relation between the initial peak density n in the 2D gas and τ:

$$n = \left(\frac{9}{\tau K}\right)^{1/2} = 5.3 \times 10^{14} \quad \mathrm{cm}^{-3}. \tag{S5}$$

Here we used the value $K = 1.1 \times 10^{-28}$ cm^{6}s^{-1} from (*26*) as the three-body loss coefficient for the $|5S_{1/2}, F = 2\rangle$ state for a classical (non-condensed) gas. This density is also consistent with the peak atom number per tube derived from the atomic temperature and trap vibrational frequencies.

Detuning dependence of the cooling sequence

We also test a few different detuning for the optical pumping beam of dRSC. For each detuning setting, the laser intensity was adjusted to maintain a scattering rate of $\Gamma_s \sim 2 \times 10^3$ s^{-1} on the $|5S_{1/2}, F = 2, m_F = 1\rangle \rightarrow |5P_{1/2}, F = 2, m_F = 2\rangle$ transition. When using exactly the same cooling sequence as described in the main text, we succeed to produce a condensate also at a the smaller detuning $\Delta_2/(2\pi) = -100$ MHz (Fig. S2**C**) but not at $\Delta_2/(2\pi) = -20$ MHz or $+40$ MHz (Fig. S2**A**-**B**).

Velocity distribution of the Z and X direction

We measure the velocity distributions of the Z and X directions with 1.3 ms ballistic expansion time (Fig. S4). It shows a bimodal velocity distribution along the vertical direction and a Gaussian distribution along the horizontal direction. Near 95% atoms are in the vibrational ground state of X (or Y) direction. The velocity (momentum) distribution is showing the Gaussian profile of the vibrational ground state.

BEC regime

For our parameters, at the critical temperature for quantum degeneracy of $k_B T \approx \hbar\omega_{xy}$, the system is at the boundary between a 3D gas and a 1D gas (*25*). Furthermore, the dimensionless interaction parameter $\gamma = mg_1/\hbar^2 n_1$ (*20*), where n_1 is the 1D density, and $g_1 \sim 2\hbar\omega_{xy}a$ is the interaction strength for the 3D scattering length a, for our system is $\gamma \approx 2.7$ at the peak 1D density. This means that the system is also at the boundary between a weakly interacting Thomas-Fermi gas ($\gamma \ll 1$, for high linear density n_1) and a strongly correlated Tonks gas ($\gamma \gg 1$, for low n_1) (*20, 23, 24*). In fact, the latter has been measured to exhibit substantially lower collisional two-body and three-body loss due to the reduced correlation function (*27, 28*). This effect may also help further reduce the light-induced loss during dRSC in the near-1D geometry. We estimate average final thermalization rate as 10^3 s^{-1}, including a factor of 5 reduction for $\gamma \approx 2.7$ (*33*), and a factor of $e^{-1.5}$ reduction for $k_B T < 2\hbar\omega_r$ (*34*).

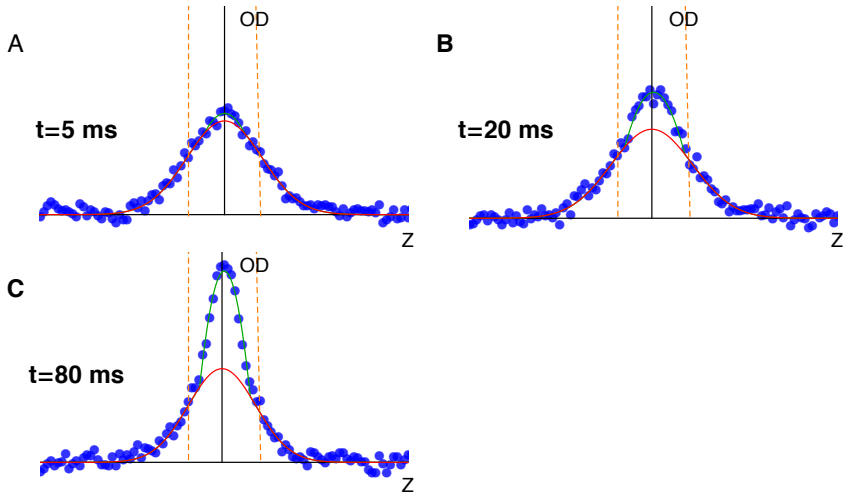

Figure S1: The method of Gaussian fit to the wings of the distribution.

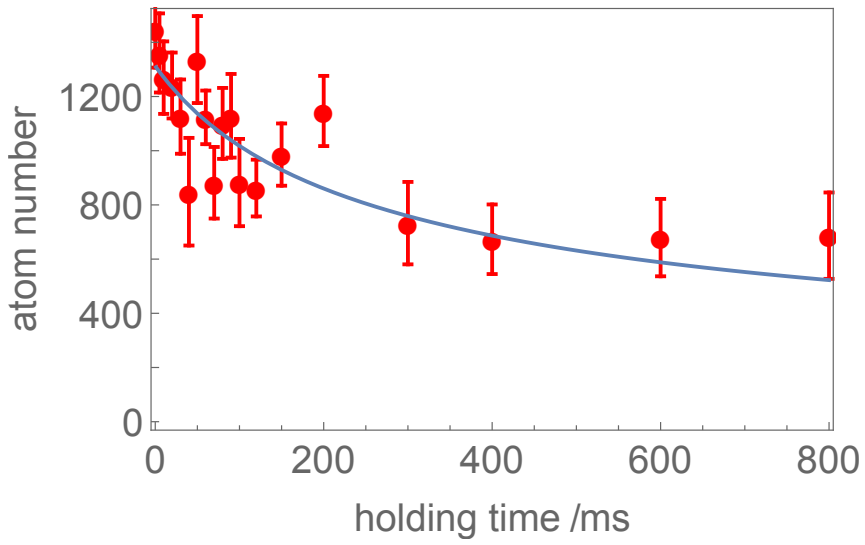

Figure S2: Atom number in the $|F = 2\rangle$ state as a function of the holding time in the Y lattice. The blue solid line is a fit to the analytic solution of the three-body loss decay, with an initial loss timescale of $\tau = 300$ ms.

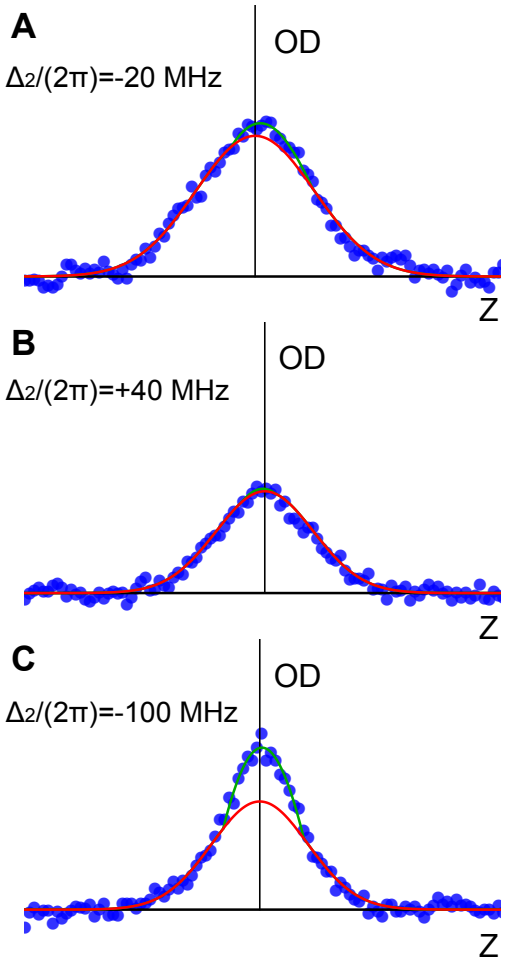

Figure S3: Velocity distribution of the atoms along the Z direction after 80 ms of cooling in the final cooling stage, for various detunings of the cooling beam $\Delta_2/(2\pi) = -20$ MHz (**A**), $\Delta_2/(2\pi) = +40$ MHz (**B**) and $\Delta_2/(2\pi) = -100$ MHz (**C**), avaraged over 100 repetitions. The data is fitted with a bimodal distribution in the same way as in Fig. 2 of the main text.

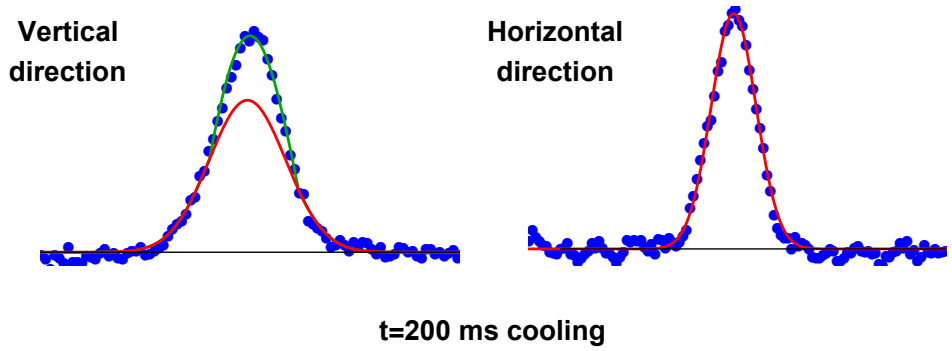

Figure S4: Velocity distribution of the Z (vertical) and X (horizontal) directions with 1.3 ms expansion time. The trap is instantaneously turned off (< 100 ns) and the final stage cooling time is 200 ms. The red line is a Gaussian fit to the wings of the distribution.

Table S1: Experimental parameters.

trap wavelength λ	1064 nm
power of each trapping beam	1.1 W
waist	18 μm
$\omega_{xy}/(2\pi)$	180 kHz
$\omega_{r2\mathrm{D}}/(2\pi)$	4.5 kHz
$\omega_z/(2\pi)$	6.3 kHz
trap depth in the 1D lattice U/h	13 MHz
magnetic field B	0.23 G
$\Delta_1/(2\pi)$	-660 MHz
$\Delta_2/(2\pi)$	-630 MHz

References and Notes

1. M. H. Anderson, J. R. Ensher, M. R. Matthews, C. E. Wieman, E. A. Cornell, Observation of Bose-Einstein condensation in a dilute atomic vapor. *Science* **269**, 198–201 (1995). doi:10.1126/science.269.5221.198 Medline

2. C. C. Bradley, C. A. Sackett, J. J. Tollett, R. G. Hulet, Evidence of Bose-Einstein condensation in an atomic gas with attractive interactions. *Phys. Rev. Lett.* **75**, 1687–1690 (1995). doi:10.1103/PhysRevLett.75.1687 Medline

3. K. B. Davis, M. Mewes, M. R. Andrews, N. J. van Druten, D. S. Durfee, D. M. Kurn, W. Ketterle, Bose-Einstein condensation in a gas of sodium atoms. *Phys. Rev. Lett.* **75**, 3969–3973 (1995). doi:10.1103/PhysRevLett.75.3969 Medline

4. B. DeMarco, D. S. Jin, Onset of Fermi degeneracy in a trapped atomic gas. *Science* **285**, 1703–1706 (1999). doi:10.1126/science.285.5434.1703 Medline

5. I. Bloch, J. Dalibard, S. Nascimbene, Quantum simulations with ultracold quantum gases. *Nat. Phys.* **8**, 267–276 (2012). doi:10.1038/nphys2259

6. K. W. Madison, F. Chevy, V. Bretin, J. Dalibard, Stationary states of a rotating Bose-Einstein condensate: Routes to vortex nucleation. *Phys. Rev. Lett.* **86**, 4443–4446 (2001). doi:10.1103/PhysRevLett.86.4443 Medline

7. S. Stellmer, B. Pasquiou, R. Grimm, F. Schreck, Laser cooling to quantum degeneracy. *Phys. Rev. Lett.* **110**, 263003 (2013). doi:10.1103/PhysRevLett.110.263003 Medline

8. T. Walker, P. Feng, Measurements of collisions between laser-cooled atoms. *Adv. At. Mol. Opt. Phys.* **34**, 125–170 (1994). doi:10.1016/S1049-250X(08)60076-2

9. K. Burnett, P. S. Julienne, K. Suominen, Laser-driven collisions between atoms in a Bose-Einstein condensed gas. *Phys. Rev. Lett.* **77**, 1416–1419 (1996). doi:10.1103/PhysRevLett.77.1416 Medline

10. S. Wolf, S. J. Oliver, D. S. Weiss, Suppression of recoil heating by an optical lattice. *Phys. Rev. Lett.* **85**, 4249–4252 (2000). doi:10.1103/PhysRevLett.85.4249 Medline

11. J. Dalibard, C. Cohen-Tannoudji, Laser cooling below the Doppler limit by polarization gradients: Simple theoretical models. *J. Opt. Soc. Am. B* **6**, 2023 (1989). doi:10.1364/JOSAB.6.002023

12. S. E. Hamann, D. L. Haycock, G. Klose, P. H. Pax, I. H. Deutsch, P. S. Jessen, Resolved-sideband Raman cooling to the ground state of an optical lattice. *Phys. Rev. Lett.* **80**, 4149–4152 (1998). doi:10.1103/PhysRevLett.80.4149

13. V. Vuletić, C. Chin, A. J. Kerman, S. Chu, Degenerate Raman sideband cooling of trapped cesium atoms at very high atomic densities. *Phys. Rev. Lett.* **81**, 5768–5771 (1998). doi:10.1103/PhysRevLett.81.5768

14. A. J. Kerman, V. Vuletić, C. Chin, S. Chu, Beyond optical molasses: 3D Raman sideband cooling of atomic cesium to high phase-space density. *Phys. Rev. Lett.* **84**, 439–442 (2000). doi:10.1103/PhysRevLett.84.439 Medline

15. J. Rührig, T. Bäuerle, A. Griesmaier, T. Pfau, High efficiency demagnetization cooling by suppression of light-assisted collisions. *Opt. Express* **23**, 5596–5606 (2015). doi:10.1364/OE.23.005596 Medline

16. M. T. DePue, C. McCormick, S. L. Winoto, S. Oliver, D. S. Weiss, Unity occupation of sites in a 3D optical lattice. *Phys. Rev. Lett.* **82**, 2262–2265 (1999). doi:10.1103/PhysRevLett.82.2262

17. D.-J. Han, S. Wolf, S. Oliver, C. McCormick, M. T. DePue, D. S. Weiss, 3D Raman sideband cooling of cesium atoms at high density. *Phys. Rev. Lett.* **85**, 724–727 (2000). doi:10.1103/PhysRevLett.85.724 Medline

18. V. Vuletić, C. Chin, A. J. Kerman, S. Chu, Suppression of atomic radiative collisions by tuning the ground state scattering length. *Phys. Rev. Lett.* **83**, 943–946 (1999). doi:10.1103/PhysRevLett.83.943

19. Supplementary materials.

20. D. S. Petrov, G. V. Shlyapnikov, J. T. M. Walraven, Regimes of quantum degeneracy in trapped 1D gases. *Phys. Rev. Lett.* **85**, 3745–3749 (2000). doi:10.1103/PhysRevLett.85.3745 Medline

21. I. Bouchoule, K. V. Kheruntsyan, G. V. Shlyapnikov, Interaction-induced crossover versus finite-size condensation in a weakly interacting trapped one-dimensional Bose gas. *Phys. Rev. A* **75**, 031606 (2007). doi:10.1103/PhysRevA.75.031606

22. P. Krüger, S. Hofferberth, I. E. Mazets, I. Lesanovsky, J. Schmiedmayer, Weakly interacting Bose gas in the one-dimensional limit. *Phys. Rev. Lett.* **105**, 265302 (2010). doi:10.1103/PhysRevLett.105.265302 Medline

23. T. Kinoshita, T. Wenger, D. S. Weiss, Observation of a one-dimensional Tonks-Girardeau gas. *Science* **305**, 1125–1128 (2004). doi:10.1126/science.1100700 Medline

24. B. Paredes, A. Widera, V. Murg, O. Mandel, S. Fölling, I. Cirac, G. V. Shlyapnikov, T. W. Hänsch, I. Bloch, Tonks-Girardeau gas of ultracold atoms in an optical lattice. *Nature* **429**, 277–281 (2004). doi:10.1038/nature02530 Medline

25. A. Görlitz, J. M. Vogels, A. E. Leanhardt, C. Raman, T. L. Gustavson, J. R. Abo-Shaeer, A. P. Chikkatur, S. Gupta, S. Inouye, T. Rosenband, W. Ketterle, Realization of Bose-Einstein condensates in lower dimensions. *Phys. Rev. Lett.* **87**, 130402 (2001). doi:10.1103/PhysRevLett.87.130402 Medline

26. J. Söding, D. Guéry-Odelin, P. Desbiolles, F. Chevy, H. Inamori, J. Dalibard, Three-body decay of a rubidium Bose–Einstein condensate. *Appl. Phys. B* **69**, 257–261 (1999). doi:10.1007/s003400050805

27. B. Laburthe Tolra, K. M. O'Hara, J. H. Huckans, W. D. Phillips, S. L. Rolston, J. V. Porto, Observation of reduced three-body recombination in a correlated 1D degenerate Bose gas. *Phys. Rev. Lett.* **92**, 190401 (2004). doi:10.1103/PhysRevLett.92.190401 Medline

28. E. Haller, M. Rabie, M. J. Mark, J. G. Danzl, R. Hart, K. Lauber, G. Pupillo, H.-C. Nägerl, Three-body correlation functions and recombination rates for bosons in three dimensions and one dimension. *Phys. Rev. Lett.* **107**, 230404 (2011). doi:10.1103/PhysRevLett.107.230404 Medline

29. Y. Castin, J. I. Cirac, M. Lewenstein, Reabsorption of light by trapped atoms. *Phys. Rev. Lett.* **80**, 5305–5308 (1998). doi:10.1103/PhysRevLett.80.5305

30. W. S. Bakr, J. I. Gillen, A. Peng, S. Fölling, M. Greiner, A quantum gas microscope for detecting single atoms in a Hubbard-regime optical lattice. *Nature* **462**, 74–77 (2009). doi:10.1038/nature08482 Medline

31. J. F. Sherson, C. Weitenberg, M. Endres, M. Cheneau, I. Bloch, S. Kuhr, Single-atom-resolved fluorescence imaging of an atomic Mott insulator. *Nature* **467**, 68–72 (2010). doi:10.1038/nature09378 Medline

32. W. Ketterle, N. J. van Druten, Bose-Einstein condensation of a finite number of particles trapped in one or three dimensions. *Phys. Rev. A* **54**, 656–660 (1996). doi:10.1103/PhysRevA.54.656 Medline

33. T. Kinoshita, T. Wenger, D. S. Weiss, Local pair correlations in one-dimensional Bose gases. *Phys. Rev. Lett.* **95**, 190406 (2005). doi:10.1103/PhysRevLett.95.190406 Medline

34. I. E. Mazets, J. Schmiedmayer, Thermalization in a quasi-one-dimensional ultracold bosonic gas. *New J. Phys.* **12**, 055023 (2010). doi:10.1088/1367-2630/12/5/055023